CHAPTER 37

PREDICTION CURVES FOR WAVES NEAR THE SOURCE OF AN IMPULSE

Robert L Miller
Department of the Geophysical Sciences
The University of Chicago

The Problem

The general problem of single-impulse induced waves has been under experimental investigation by the author for several years The present paper is confined to a presentation of the wave modes which are to be expected for various permutations of displacement velocity and displacement length at the impulse source Other portions of the study will be published elsewhere

It is clear that a number of geometric arrangements in the laboratory may be made to generate impulse waves, for example, sudden upthrust or downdrop of a block on the tank bottom analagous to block faulting on the sea-floor in nature, or a hinged flap moving on the bottom analagous to the undulatory bottom motion which may occur during seismic disturbances on the sea floor However, it is my opinion that the impulse generator which is most simple and most easily related to contemporary generalized theory, is a single piston thrust at one end of the wave tank which pushes the fluid down channel (See Figure 1) As an additional simplification, the investigation is carried out for the flat bottom, fixed depth case, relegating the effect of varying depth to a later study

The parameters of the impulse may thus be adequately described by the dimensionless variables ℓ/d (where ℓ is distance the pistion is displaced, and the constant, d, is the undistured water depth) and a piston Froude number $\bar{V}/\sqrt{gd}$ (where $\bar{V}$ is the piston speed and $\sqrt{gd}$ is the long wave velocity The range of dimensionless piston displacements and piston velocities were chosen to cover reasonably well (where information is available), the movements of natural impulse generators This includes coastal landslides entering a body of water, iceberg calving, seismic movements of various kinds, and explosions None of the types of natural impulse generators referred to above are clearly modeled by a horizontal piston motion, although in many cases, the resultant of the natural motion may fit rather well, thus indicating the generality of this simple model

Permutations of ℓ/d and $\bar{V}/\sqrt{gd}$ (or $F_{\bar{V}}$) through the selected range yields a series of points on the ℓ/d, $F_{\bar{V}}$ plane If a ℓ/d, $F_{\bar{V}}$ plane is fixed at some arbitrary distance from the end of the piston motion, each point on the plane may be further described in terms of wave mode, some sort of wave speed, wave amplitude, etc If a single wave is tracked down channel, it will be indicated by a fixed point on the ℓ/d, $F_{\bar{V}}$ plane representing initial generating conditions However, the nature of the wave mode, and the magnitude of wave speed and amplitude will change during the transformations which occur as the impulse wave progresses down channel Thus, although the position of the point on the ℓ/d, $F_{\bar{V}}$ plane does not change for a series of distances from the piston, the value or nature of the parameters for that point, will change This yields a series of graphs consisting of ℓ/d, $F_{\bar{V}}$ planes at various fixed distances from the piston, which indicate the changes in wave mode, Froude number and maximum amplitude (Figures 5, 6 and 7)

Since the impulse waves are undergoing transformations and decay as they progress down channel, the question of a meaningful velocity must be considered In this study, two velocities are measured The first is a "phase velocity" A fixed point on the wave profile is tracked on multichannel oscillograph records It is assumed that the transformations take place slowly relative to the short distance between two recording stations, and that the error in this approximation is not large This method which yields an average velocity between points approximately 2 5 meters apart is in maximum error in the bore range near the piston where transformation is rapid and improves down channel Thus, 2 5 meters is regarded as a characteristic "transformation distance" for these wave channel experiments The Froude number representing this measurement of velocity is referred to as $F_{\bar{C}}$, and the results are shown in Figure 6

The second velocity in this study is the Boussinesq (1872) velocity of propagation of a volume element of the impulse wave We have succeeded in devising an electronic system which will measure this velocity but due to space limitations, the method and results must be published elsewhere

Sensing and Recording System

The surface time history of the impulse waves is obtained through capacitance probe sensors at a series of stations along the channel (Figure 2, D) The wave sensor is basically an amplitude modulated square wave generator As the probe is immersed in the fluid, the capacitance increases, resulting in a modulated envelope directly proportional to the instantaneous degree of immersion For details see L F McGoldrick, 1969

The probe is constructed of #17 gage hypodermic tubing with a polyethylene sleeve (O D 1 194 mm) forming the dialectric (Figure 3a) Capacitive sensitivity is 20 pfd/cm giving a signal sensituity of 0 5 V/cm

The probe unit is driven by a 20 V D C power supply The wave information in D C volts from the probe actlvates an operational amplifier (Fig 2,C and Fig 3) programmed as a subtracting amplifier, deleting the signal due to static water level (Fig 2,A), and also serving as the resultant output sensitivity control (Fig 2,E) This proved to be very useful when the experiments required an array of probes, and led to standardized calibration for all probes The signal from the subtracting amplifier activates an oscillograph recorder for graphic analysis of wave properties (Figure 4)

The signal from the subtracting amplifier also goes to a second operational amplifier programmed to interact with a capacitor to perform a graphic integration of the wave amplitude (Fig 2,B and Fig 3) The output from this unit activates an oscillograph recorder for graphic analysis of the wave volume (Figure 4) A ramp control is used to offset potential that may have accumulated in the integrator unit before the arrival of the wave

This brief summary given in this section will be considerably amplified in a forthcoming technical report, White and Miller, Tech Rept No 10, 1970

Results

Figure 5 shows the changes in wave mode as a function of distance from the impulse source Four initial wave modes are recognized These are, in order of increasing initial energy with the lowest first, "sinusoid", "solitary",[1] "undular bore" and fully developed bore (See Figure 4)

The following conclusions are drawn

1 The fully developed bore decays rapidly to the unbroken undular bore form (Figs 5, 6, 7)

2 The lead wave of the undular form takes on the "solitary" mode leaving behind the rest of the "undular" wave In several cases, the second and even the third undulations in turn take on the "solitary" mode (Figs 5e,f)

3 The "sinusoid" mode generated at short piston displacements transforms gradually as the trailing trough rises to the undisturbed water level, and finally enters the "solitary" mode (Figs 5a-f)

---

[1] The term "solitary" is applied to the stable, symmetrical form which satisfies the following conditions

1) both leading and trailing portions asymptotically approach the static level

2) phase velocity agreed well with Laitone's 1961 wave speed equation taken to the first three terms $C = \sqrt{gd}\ (1 + \frac{1}{2}\frac{H}{d} - \frac{3}{20}(\frac{H}{d})^2 +$

3) amplitude as a function of volume, agrees well with the relationship given by Kuelegan and Patterson, 1940 $h_1 = \frac{3Q^2}{16H^3}$ where h_1 is max amp , Q is cross-sectional area, and H is static water depth

4 The Froude number[2] gradient indicates no striking irregularities, and indicates that all wave modes are in the breaking regime at approximately $F_{\bar{C}}$ = 1 26 (Figure 6)

5 The experimentally established line dividing the breaking region from the unbroken region seems to be independent of wave mode The breaking wave region occupies about half of the l/d, $F_{\bar{V}}$ plane very near the impulse source at D/d = 10 and decreases steadily toward the upper right corner at D/d = 188 (Figure 5)

6 There appears to be no alternative to the conclusion that given a predictable distance down channel from the impulse source, all impulse waves will assume the "most stable" mode in agreement with the predicition of Boussinesq, 1872, i e the "solitary" form has the minimum "moment of instability" and in agreement with the discussion in Keulegan and Patterson, 1940 p 87

7 The decay sequence for a fully developed bore at the impulse source is Bore ⟶ undular bore ⟶ lead undulation becomes solitary, + trailing undular bore consisting of remaining undulations ⟶ lead undulation solitary + second undulation becomes solitary ⟶ in several runs three successive solitary forms have emerged from the preceeding undular form

Discussion

The graphs given in Figures 5, 6 and 7 form a relatively complete set of prediction curves for waves created by a horizontal impulse, surface to bottom From these graphs, it is possible to predict the wave type, maximum wave amplitude, and maximum "phase speed" for any impulse wave within the estimated natural impulse generating range These are open ended predictions, however For example, the published ℓ/d for "Shot Baker" at Bikini in the late 1940's is approximately 5 5 (Johnson and Bermel, 1949) The $F_{\bar{V}}$ value is undoubtedly very high but not available In the landslide case, I have estimated ℓ/d to be about 8 0 based on examination of landslide scars on coastal charts, if one takes avalanche figures for displacement velocity, the $F_{\bar{V}}$ values may easily exceed 40 0 Large scale seismic movements are particularly difficult to estimate, but for a submarine overthrust, ℓ/d less than 1 0 and $F_{\bar{V}}$ less than 0 3 may be reasonable In general, natural impulses yielding ℓ/d values in excess of 9 0 coupled with $F_{\bar{V}}$ greater than 1 0

[2] Since this Froude number is based on an average phase velocity, it is insensitive to changes in velocity over the wave profile during transformations I have found that the Boussinesq velocity on the other hand does bring out these changes quite clearly

should not change the pattern of the prediction graphs The wave mode will be either an undular bore or fully developed bore, with the same transition and decay sequence found in this study, differing only in magnitude I feel extrapolation in this sense is justified The very low ℓ/d high $F_{\bar{V}}$ corner of the graphs is a different matter My present generating system will not produce impulses in this region It would appear that some other sort of impulse generating mechanism should be devised for this region of the ℓ/d, $F_{\bar{V}}$ plane

Finally, it seems suggestive that the linear theoretical models for impulse waves of the type discussed in Lamb (1932, Art 238ff) are inadequate For example, Cauchy-Poisson wave trains are not generated by this type of impulse mechanism in which the initial conditions include a velocity and surface elevation This is in clear contrast to the experiments of Prins 1958 where the initial conditions include a surface elevation but no initial velocity It is interesting to note that Prins found wave modes similar to those described in this paper but also for the low energy impulse, obtained an oscillatory wave region of the Cauchy-Poisson type It is possible that a similar type of wave may exist in the low ℓ/d very high $F_{\bar{V}}$ region (Figure 5) which in my study was not investigated Further development of the more realistic non-linear models, Perigrine 1968, 1969, is required to fit the "real" case

Acknowledgements are due to Robert V White who is responsible for a major portion of the sensing and recording system, to L F McGoldrick for advice and comment on almost all phases of the study, and to J M Witting for several illuminating discussions This study was supported by the Office of Naval Research Geography Branch, N0014-67-A-0285-0013

Bibliography

Boussinesq, J Theorie des ondes etc Liouville's Jour Vol 17, 1872

Johnson, J W and K J Bermel Impulsive waves in shallow water as generated by falling weights Trans A G U V 30, No 2, April, 1949, pp 223-230

Kuelegan, G H and G W Patterson Mathematical theory of irrotational translation waves Jour of Res of Nat Bur Standards , Vol 24, R P 1272, 1940

Laitone, E V Higher approximation to non-linear water waves and the limiting heights of Cnoidal, Solitary and Stokes waves Inst of Eng Res Tech Rept 89-6, Berkeley, Calif ,1961

Lamb, H Hydrodynamics, 6th Edition, Dover Press (1st' Ed) 1932

McGoldrick, L F A system for the generation and measurement of capillary-gravity waves Office of Naval Research, Tech Rept No 3, August 1969

Miller, R L and R V White A single impulse system for generating solitary, undulating surge and gravity shock waves in the laboratory Tech Rept No 5, Fluid Dynamics Lab , Dept Geophys , Univ of Chicago, 1966

Perigrine, D H Long waves in a channel of arbitrary cross-section Jour Fluid Mech 32, 353-365, 1968

Ibid, Solitary waves in trapezoidal channels Jour Fluid Mech 35, 1-6, 1969

Prins, J E Characteristics of waves generated by a local disturbance Trans A G U Oct 1958 pp 865-874

White, R V and R L Miller An electrical system for sensing and analysing wave properties including integration and differentiating capability Tech Rept No 10, Fluid Dynamics Lab , Dept Geophys Sci , Univ of Chicago (In press)

Figure Captions

FIGURE

1 Schematic of wave generating and wave sensing system For details of the wave tank facility see Miller & White, 1966

2 Flow sheet for wave recording and integrating systems

3 Detailed schematic of operational amplifiers, wave recording and integrating

3a Capacitance probe unit for sensing waves

4 The four possible wave modes due to a single horizontal impulse The cross-sectional area of fluid displaced by the piston is matched against the cumulative curve (integration over wave height) B in the figure This produces a cut-off point (A) on the wave trace where the cross-sectional area under the wave trace is equivalent to the cross sectional area of the fluid volume at the impulse source due to the several damped back and forth oscillations which occur after the magnetic brake has been applied

5 a,b,c,d,e,f The wave mode field as a function of impulse displacement ℓ/d and speed of displacement in Froude number form $F_{\bar{V}}$ or ($\bar{V}/\sqrt{gd}$) for fixed distances from the impulse source ℓ is piston displacement d is undisturbed water depth D is distance from impulse source and $\bar{V} = \ell/t$ where t is elapsed time during piston displacement Note that in 5a at D/d = 10 closest to the source, there is no "solitary" wave region, whereas the "solitary" region is significant D/d = 65, and dominant at D/d = 150

6 a,b,c Froude number gradient, $F_{\bar{V}}$, superimposed on the wave mode field at D/d ≈ 10, 65, 150 Note that the breaking region retreats steadily toward the upper right corner with increase in distance from impulse source, and that the breaker line always lies between $F_{\bar{V}}$ = 1 25 and 1 30

7 a,b,c Maximum wave amplitude gradient superimposed on wave mode field for D/d = 10, 65, 150 Because of the relatively coarse contour interval, the abrupt drop in maximum amplitude from smooth to breaking appears only in Fig 7b, at D/d = 65

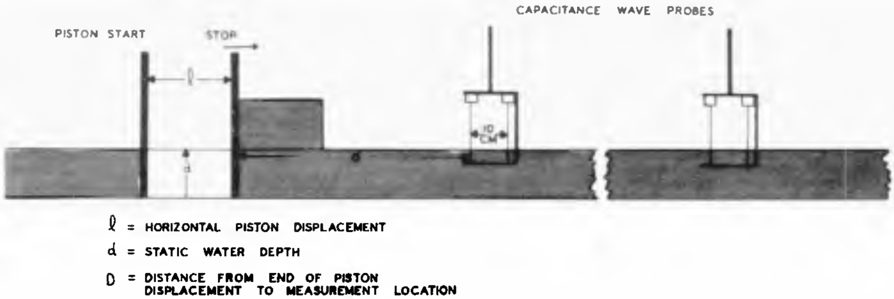

CAPACITANCE WAVE PROBES
PISTON START
STOP
10 CM
ℓ = HORIZONTAL PISTON DISPLACEMENT
d = STATIC WATER DEPTH
D = DISTANCE FROM END OF PISTON DISPLACEMENT TO MEASUREMENT LOCATION

Fig. 1

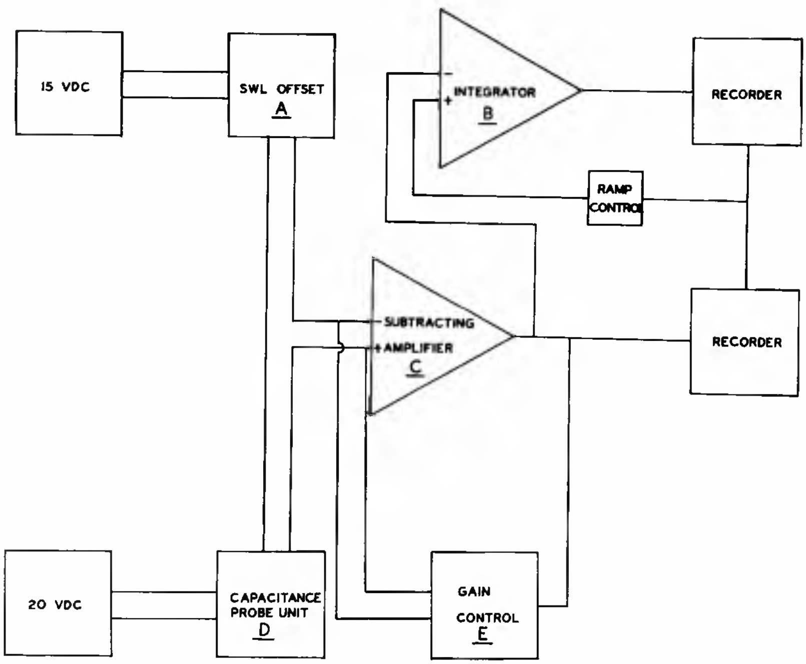

15 VDC
SWL OFFSET A
INTEGRATOR B
RECORDER
RAMP CONTROL
SUBTRACTING AMPLIFIER C
RECORDER
20 VDC
CAPACITANCE PROBE UNIT D
GAIN CONTROL E

Fig. 2

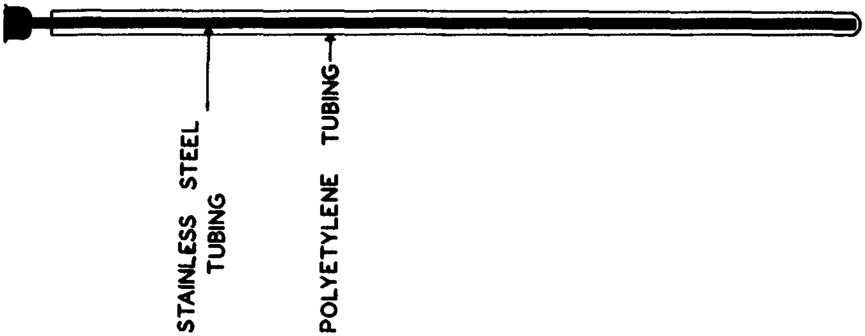
STAINLESS STEEL TUBING
POLYETYLENE TUBING

Fig 3a

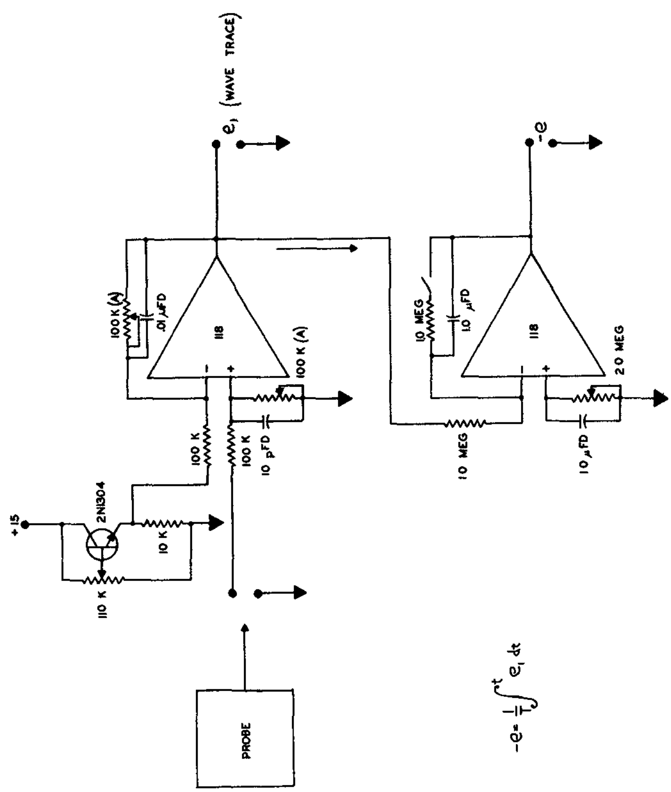
PROBE
+15
2N1304
110 K
10 K
100 K
100 K
10 pFD
118
100 K (A)
.01 μFD
100 K (A)
e_1 (WAVE TRACE)
10 MEG
10 MEG
1.0 μFD
118
20 MEG
10 μFD
-e
$-e = \frac{1}{T}\int^t e_1\,dt$

Fig 3

WAVE MODES

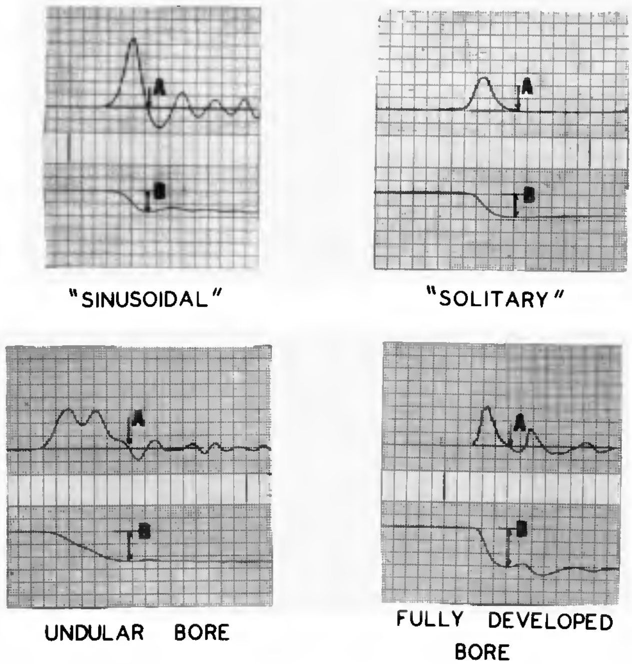

Fig. 4

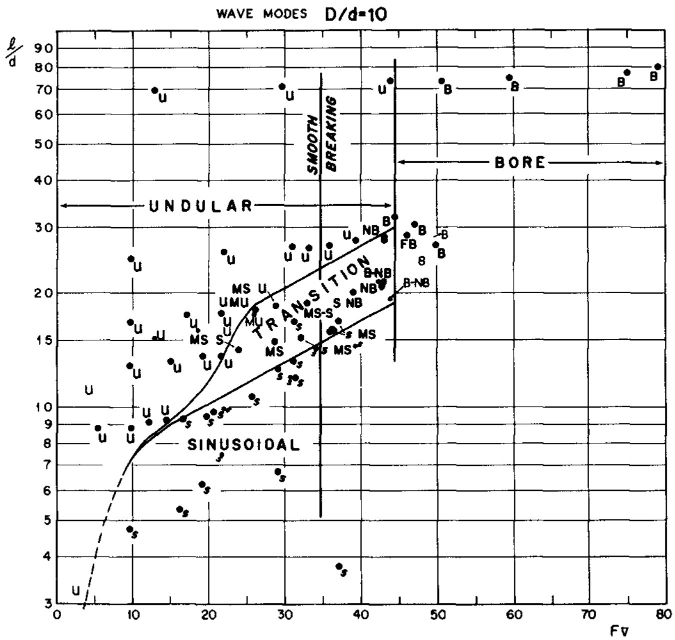
WAVE MODES D/d=10
l/d
SMOOTH
BREAKING
BORE
UNDULAR
TRANSITION
SINUSOIDAL
Fv

Fig 5a

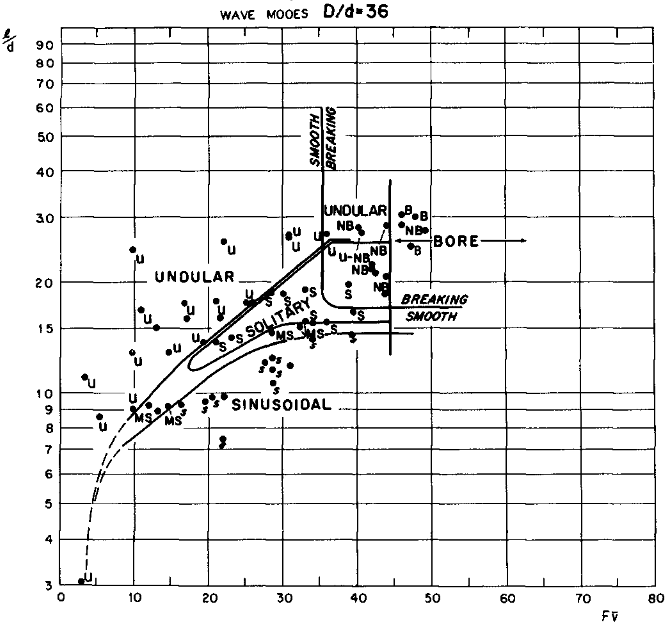
WAVE MODES D/d=36
l/d
SMOOTH
BREAKING
UNDULAR
BORE
SOLITARY
SINUSOIDAL
BREAKING
SMOOTH
Fv

Fig 5b

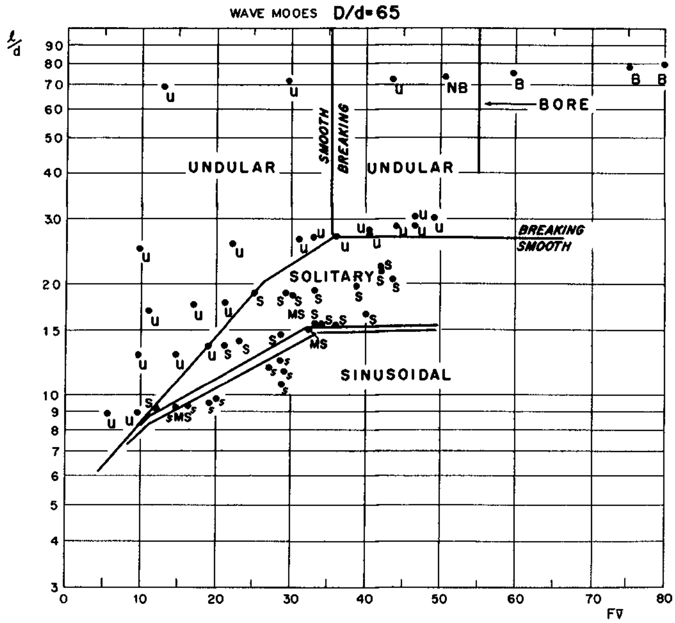
WAVE MODES D/d=65
l/d
UNDULAR
SMOOTH
BREAKING
UNDULAR
BORE
NB
B
BREAKING
SMOOTH
SOLITARY
SINUSOIDAL
FV

Fig 5c

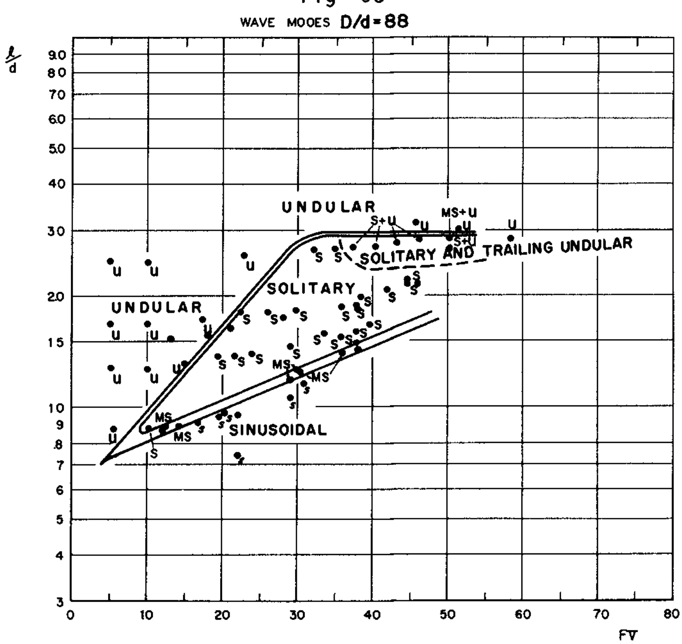
WAVE MODES D/d=88
l/d
UNDULAR
MS+U
S+U
SOLITARY AND TRAILING UNDULAR
SOLITARY
UNDULAR
SINUSOIDAL
FV

Fig 5d

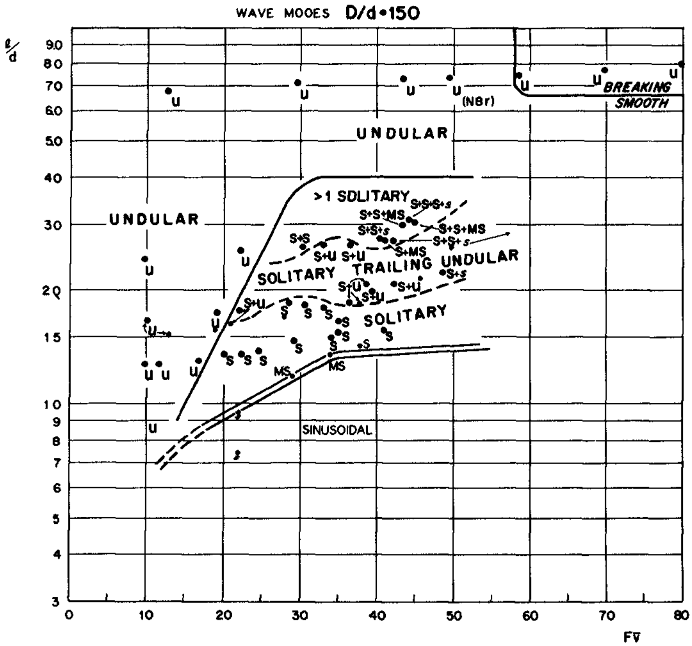
WAVE MODES D/d=150
ℓ/d
FV
UNDULAR
>1 SOLITARY
SOLITARY TRAILING UNDULAR
SOLITARY
SINUSOIDAL
BREAKING
SMOOTH
(NBr)

Fig 5e

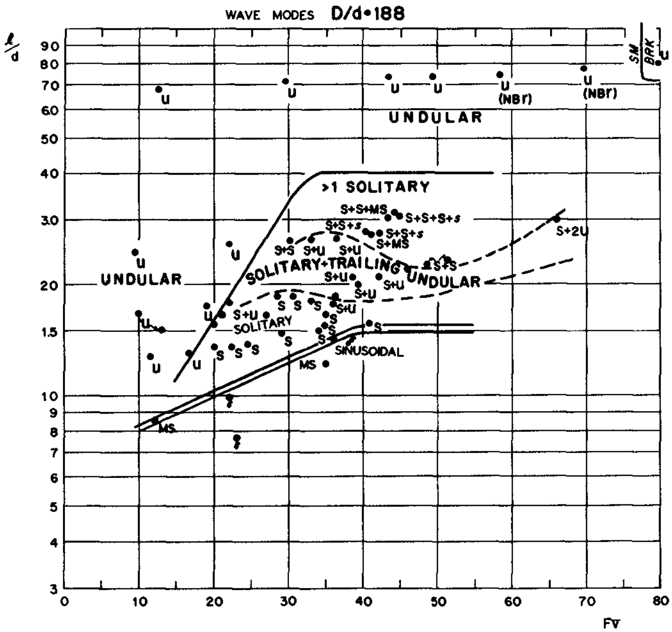
WAVE MODES D/d=188
ℓ/d
FV
UNDULAR
>1 SOLITARY
SOLITARY+TRAILING UNDULAR
SOLITARY
SINUSOIDAL
SM
BRK
(NBr)

Fig 5f

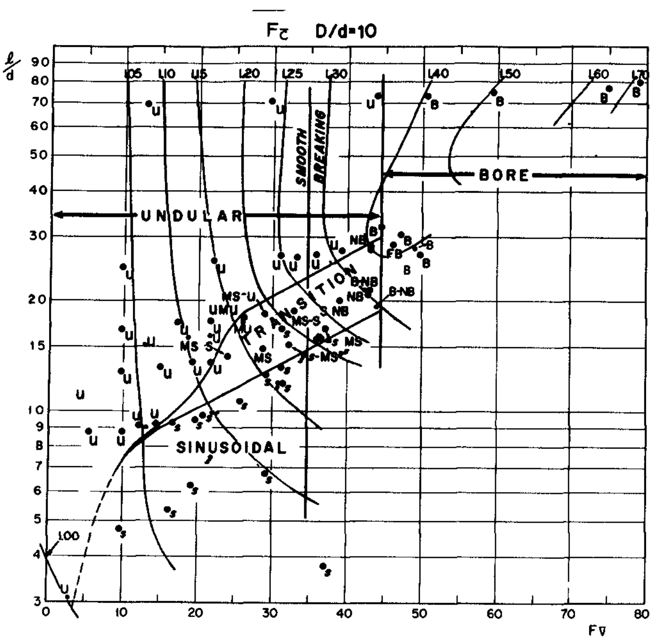
Fc D/d=10
l/d
Fv
UNDULAR
BORE
SMOOTH
BREAKING
TRANSITION
SINUSOIDAL

Fig 6a

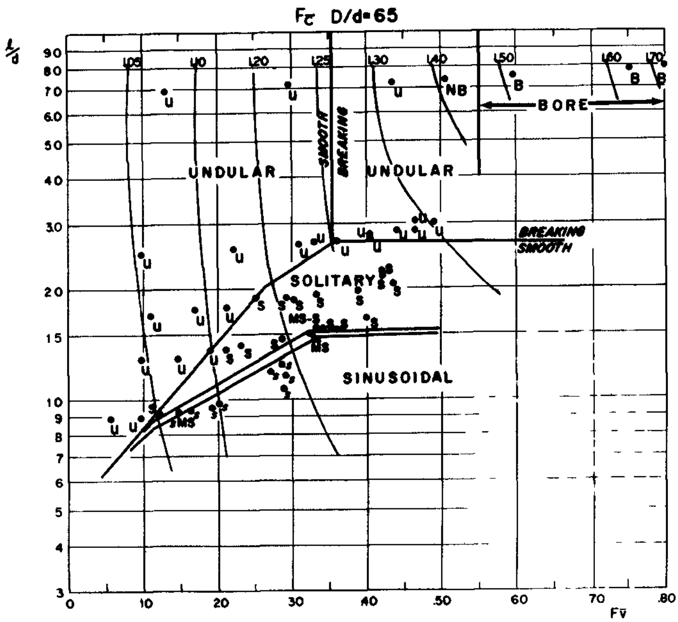
Fc D/d=65
l/d
Fv
UNDULAR
UNDULAR
BORE
SMOOTH
BREAKING
SOLITARY
SINUSOIDAL

Fig 6b

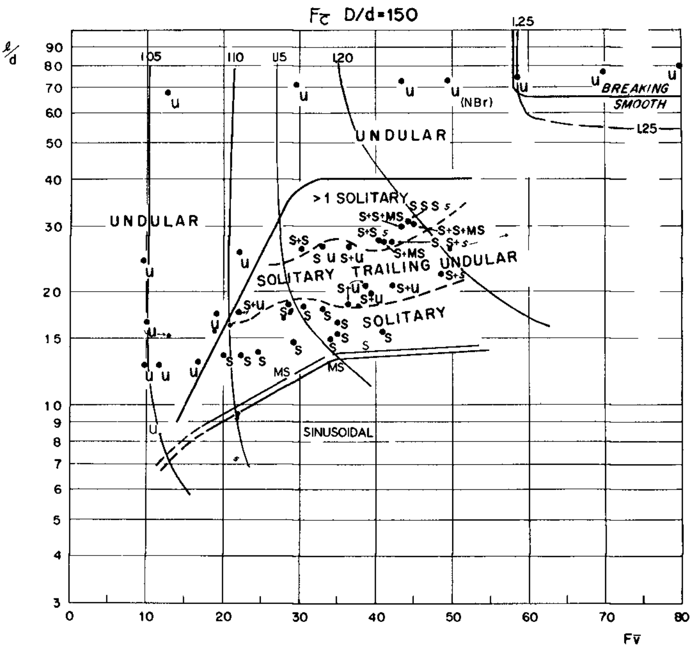
$F_{\overline{\tau}}$ D/d=150
ℓ/d
1.05
1.10
1.15
1.20
1.25
UNDULAR
BREAKING
SMOOTH
(NBr)
>1 SOLITARY
SOLITARY
TRAILING UNDULAR
SOLITARY
SINUSOIDAL
MS
$F_{\overline{V}}$

Fig 6c

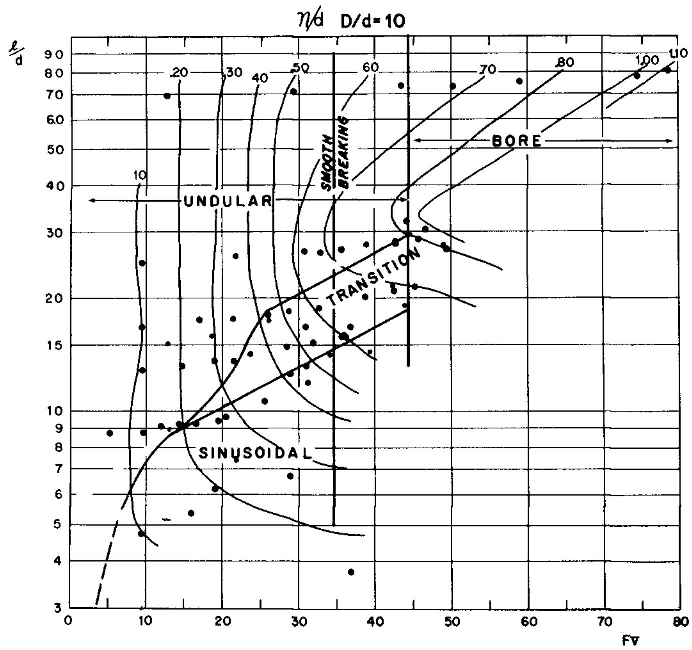
η/d D/d=10
ℓ/d
.10
.20
.30
.40
.50
.60
.70
.80
1.00
1.10
SMOOTH
BREAKING
BORE
UNDULAR
TRANSITION
SINUSOIDAL
$F_{\overline{V}}$

Fig 7a

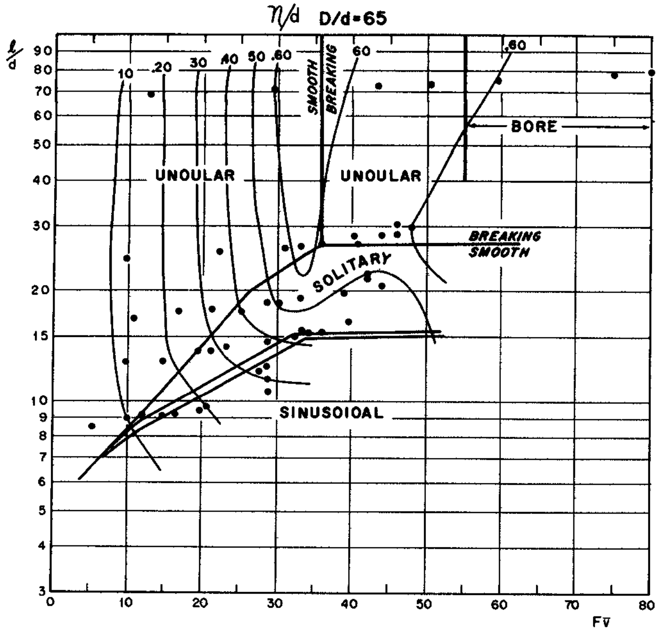
η/d D/d=65
ℓ/d
UNOULAR
UNOULAR
SMOOTH
BREAKING
BORE
BREAKING
SMOOTH
SOLITARY
SINUSOIOAL
Fv

Fig 7b

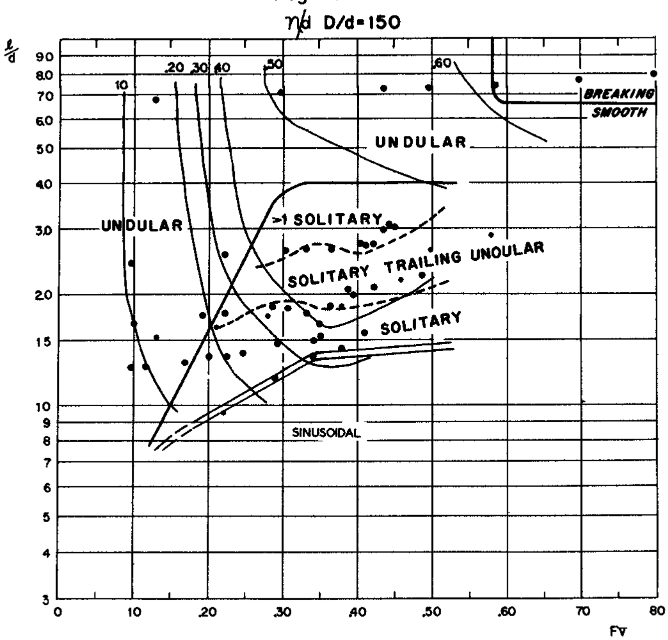
η/d D/d=150
ℓ/d
UNDULAR
UNDULAR
BREAKING
SMOOTH
>1 SOLITARY
SOLITARY TRAILING UNOULAR
SOLITARY
SINUSOIDAL
Fv

Fig 7c